MALAYSIAN JOURNAL OF MICROSCOPY

Journal homepage: https://malaysianjournalofmicroscopy.org

RESEARCH ARTICLE

MORPHOLOGICAL AND MECHANICAL CHARACTERISTICS OF DENSE POROUS CERAMICS USING CARBON BLACK AND POLYMETHYL METHACRYLATE AS PORE-FORMING AGENTS AT VARYING CONCENTRATIONS

Mohamed Lokman Jalaluddin, Umar Al-Amani Azlan*, Mohd Warikh Abd Rashid

Fakulti Teknologi Dan Kejuruteraan Industri Dan Pembuatan, Universiti Teknikal Malaysia Melaka, 76100, Durian Tunggal, Melaka, Malaysia.

Abstract. Porous ceramics are widely used in high-performance engineering applications due to their unique porosity, mechanical stability, and thermal resistance. However, optimizing the trade-off between porosity and mechanical strength remains a significant challenge, particularly when employing different pore-forming agents. This study investigates the morphological and mechanical characteristics of dense porous ceramics fabricated using carbon black (CB) and polymethyl methacrylate (PMMA) as pore-forming agents at varying concentrations (1–5 wt%). Despite extensive research on individual porogens, a comparative analysis of their influence on microstructure evolution, pore distribution, and mechanical performance in a single ceramic system remains largely unexplored. Ceramic samples were synthesized via a solid-state reaction and subjected to controlled sintering at 1175°C. Microstructural characterization using Field emission scanning electron microscopy (FESEM) revealed that CB generated small, uniformly distributed closed pores, enhancing mechanical integrity, while PMMA introduced larger, interconnected open pores, promoting higher porosity but reducing strength. X-ray diffraction (XRD) analysis confirmed the presence of orthoclase, silicon dioxide, and mullite phases, with variations in crystallinity influenced by porogen type. Mechanical evaluation through three-point flexural testing demonstrated that 3 wt% CB resulted in the highest flexural strength of 49.72 MPa, whereas PMMA incorporation led to a substantial decrease, reaching 14.80 MPa at 5 wt% due to excessive porosity and structural discontinuities. This study provides new insights into porogen selection for tailoring ceramic microstructures, demonstrating that CB is more suitable for applications requiring high mechanical strength, while PMMA is beneficial where enhanced permeability is prioritized. The findings contribute to the development of high-performance porous ceramics for energy-efficient insulation, filtration, and lightweight structural applications, offering a systematic framework for optimizing porosity-mechanical strength relationships in advanced ceramic materials.

Keywords: Porous ceramics, carbon black, polymethyl methacrylate, mechanical properties, microstructure.

Article Info

Received 31 December 2024
Accepted 28 February 2025
Published 2 June 2025

***Corresponding author: umar@utem.edu.my**

ISSN: 1823-7010, eISSN: 2600-7444

1. INTRODUCTION

Porous ceramics have attracted significant interest in engineering applications due to their ability to combine low density, high thermal stability, corrosion resistance, and mechanical durability [1, 2]. These properties make them highly suitable for thermal insulation, filtration systems, catalyst supports, and biomedical scaffolds, where controlled porosity is essential for functional performance [3]. The introduction of tailored porosity in ceramics is achieved through the incorporation of porogens, which control the pore size, distribution, and morphology during processing. Among the commonly used porogens, carbon black (CB) and polymethyl methacrylate (PMMA) stand out due to their distinctive thermal decomposition behaviour and pore-forming efficiency [4]. CB, a carbonaceous material with a fine particle size of approximately 30 – 50 nm, decomposes at a higher temperature (500 °C – 700 °C), typically resulting in small, uniformly distributed closed pores, which enhances mechanical strength. In contrast, PMMA, a synthetic polymer, decomposes at a lower temperature (250 °C – 400 °C) and generates larger, interconnected pores, leading to higher porosity but reduced mechanical integrity [5, 6]. However, a direct comparative analysis of CB and PMMA in a single ceramic system remains largely unexplored.

The mechanical properties of porous ceramics are highly dependent on pore morphology, with key factors such as pore size, shape, and connectivity significantly influencing flexural strength, fracture toughness, and thermal performance [7, 8]. While numerous studies have investigated individual porogens, most research has either focused solely on morphological properties (pore size and distribution) or mechanical behaviour (strength and toughness) without establishing a clear correlation between these two essential aspects [1, 9]. A deeper understanding of how CB and PMMA influence the microstructure-mechanical property relationship is critical in optimizing porous ceramics for structural and functional applications. Moreover, the role of porogen selection in phase composition and crystallinity evolution during sintering remains underexplored, raising questions about how different porogens influence the ceramic matrix's structural integrity and thermal stability [10]. This gap in knowledge limits the ability of engineers and manufacturers to precisely control porosity while maintaining mechanical strength, a critical challenge in industries where both high porosity and structural durability are required, such as in energy-efficient insulation, lightweight structural components, and filtration media.

This study aims to address these limitations by conducting a systematic comparative investigation on the morphological and mechanical characteristics of porous ceramics produced using CB and PMMA as porogens. Specifically, the study seeks to analyze the effect of porogen type and concentration (1–5 wt%) on pore structure and mechanical performance. Additionally, the research established correlations between porogen-induced microstructural modifications and the resulting mechanical properties to provide a comprehensive framework for optimizing porous ceramics. By employing FESEM, this study offered insights into microstructural evolution, while XRD analysis helped evaluate whether porogen selection influences the phase composition and crystallinity of sintered ceramics [2]. Furthermore, mechanical testing through three-point flexural strength analysis provided a quantitative assessment of how porosity impacts mechanical integrity, ensuring a holistic understanding of porogen behaviour in ceramic processing [8].

The significance of this study lies in its practical implications for engineering applications. The findings enabled manufacturers to strategically select porogens based on their ability to optimize porosity while maintaining mechanical stability [3]. In industries where lightweight, thermally efficient, and structurally resilient ceramics are required, such as aerospace, biomedical implants, and advanced filtration systems, the ability to finely tune pore characteristics is of paramount importance [9]. This research provided a scientific basis for the rational design of porous ceramics, contributing to the development of next-generation materials with enhanced mechanical robustness and tailored porosity for high-performance applications [10].

2. MATERIALS AND METHODS

2.1 Materials

The raw materials used for ceramic synthesis comprised kaolinite, $Al_2Si_2O_5(OH)_4$ (Anji Runxing New Materials Co., Ltd., China), silicon dioxide, SiO_2 (CABOT Corporation, USA), and feldspar $KAlSi_3O_8$ (Multifilla^{TM}, Malaysia). These materials were selected based on their chemical composition and their role in ceramic densification and phase formation. The ceramic precursor was formulated with kaolinite, silica, and feldspar in mass fractions of 43.28 g, 10.07 g, and 46.65 g, respectively, maintaining a total batch weight of 100 g.

Carbon black (CB) and polymethyl methacrylate (PMMA) were employed as pore-forming agents at varying weight percentage (1–5 wt.%). CB, with a particle size distribution of 30–50 nm, was selected for its ability to generate fine, interconnected pores upon thermal decomposition. PMMA, with a particle size range of 10–20 μm, was used for its capacity to produce larger, more spherical pores. The purity and particle size distribution of CB and PMMA were verified using laser diffraction particle size analysis prior to incorporation into the ceramic matrix. Both pore-forming agents were sourced from CABOT Corporation, USA

2.2 Sample Preparation

The ceramic powders were homogenized via mechanical mixing before compaction. Initially, 1 g of dry ceramic powder was uniaxially pressed at 20 MPa for 60 s in a 13 mm stainless steel die to form the dense top layer of the bi-layered ceramic disc. Subsequently, a mixture of ceramic powder and a designated amount of pore-forming agent was placed into the mould and subjected to the same compaction conditions to form the porous bottom layer.

For mechanical characterization, rectangular bar samples (75 mm × 10 mm × 5 mm) were prepared using a similar bi-layered approach. The powders were compacted under uniaxial pressure (20 MPa, 60 s) using a steel mould to ensure uniform density distribution. The prepared green bodies were dried at 100 °C for 12 h in a laboratory oven before sintering in a high-temperature furnace (Nabertherm LHT 02/17 LB, Germany). The sintering cycle consisted of a controlled heating rate of 5°C/min up to 1175 °C, followed by a dwell time of 3 h and subsequent cooling to ambient temperature.

2.3 Material Characterizations

2.3.1 Microstructural Analysis

Field emission scanning electron microscopy, FESEM (Hitachi Schottky FESEM SU5000) was utilized to examine the microstructure, pore morphology, and distribution of the sintered ceramics. Cross-sections of the samples were polished using alumina suspension (0.5 μm) and sputter-coated with a thin gold layer to prevent charging effects. Micrographs were captured at magnifications ranging from 500x to 10,000x under an accelerating voltage of 15 kV.

2.3.2 Phase Analysis

X-ray diffraction (XRD) analysis was conducted using an X'Pert PRO diffractometer (PANalytical, Netherlands) with Cu-Kα radiation (λ = 1.5406 Å) to identify the crystalline phases present in the sintered ceramics. The scanning range was set between 10° and 80° 2θ with a step size of 0.02°.

2.3.3 Mechanical Properties

Flexural strength testing was performed using a three-point bending method by ASTM C1161 standards. The measurements were conducted on a universal testing machine (Shimadzu Autograph AG 25TA, Japan) with a crosshead displacement rate of 1 mm/min. The specimens were positioned such that the porous layer was at the bottom, ensuring stress distribution analysis between the dense and porous regions. A total of 30 samples (15 with CB and 15 with PMMA) were tested to evaluate the impact of pore-forming agents on mechanical integrity. By integrating these characterization techniques, the influence of CB and PMMA on the microstructural evolution and mechanical performance of porous ceramics was systematically analyzed.

3. RESULTS AND DISCUSSION

3.1 Microstructural Evaluation of Dense Porous Ceramics Using FESEM

The microstructural evaluation of dense porous ceramics synthesized using CB as a pore-forming agent was conducted via FESEM to analyse the evolution of porosity and morphological characteristics. The FESEM micrographs as shown in Figure 1 reveal spherical pores dispersed within the ceramic matrix, indicating the efficacy of CB as a sacrificial pore-forming agent and the magnification of the FESEM images is 500x. However, the relationship between CB content and porosity does not exhibit a strictly linear trend. Notably, while an increase in CB concentration from 1 wt% to 3 wt% results in greater pore formation (Figure 1(a) to (c)), at 4 wt% CB (Figure 1(d)), the number of pores appears to decrease compared to 3 wt%, suggesting a non-linear dependence of porosity on CB content. This phenomenon may be attributed to the coalescence of smaller pores or the partial collapse of the porous structure due to excessive burnout of the organic phase during sintering. Previous studies have reported similar non-monotonic porosity trends when employing CB as a porogen in ceramic systems, where optimal porosity is achieved within a specific concentration range before structural densification occurs [11-13]. Furthermore, the pore morphology in the synthesized ceramics exhibits a relatively uniform distribution with minimal interconnection, which aligns with findings in porous alumina systems using carbon-based templates [14]. These microstructural insights are crucial in tailoring the porosity of bi-layered ceramics for energy rationalization applications, ensuring an optimal balance between thermal conductivity and mechanical integrity.

The formation of open and closed pores in dense porous ceramics synthesized using CB as a pore-forming agent exhibits a distinct trend, as illustrated in Figure 2. At lower CB concentrations (1–2 wt%), the ceramic microstructure is characterized by a higher proportion of closed pores, which are formed due to incomplete burnout of the pore-forming agent during sintering. These closed pores are typically spherical and isolated within the matrix, resulting from the entrapment of gases released during CB decomposition [15]. As the CB concentration increases, an increase in open porosity is observed, particularly at 5 wt%, where interconnected pore networks become more prominent. The shift from predominantly closed to open porosity is attributed to the percolation threshold, where the accumulation of CB particles creates a continuous porous structure upon burnout [4].

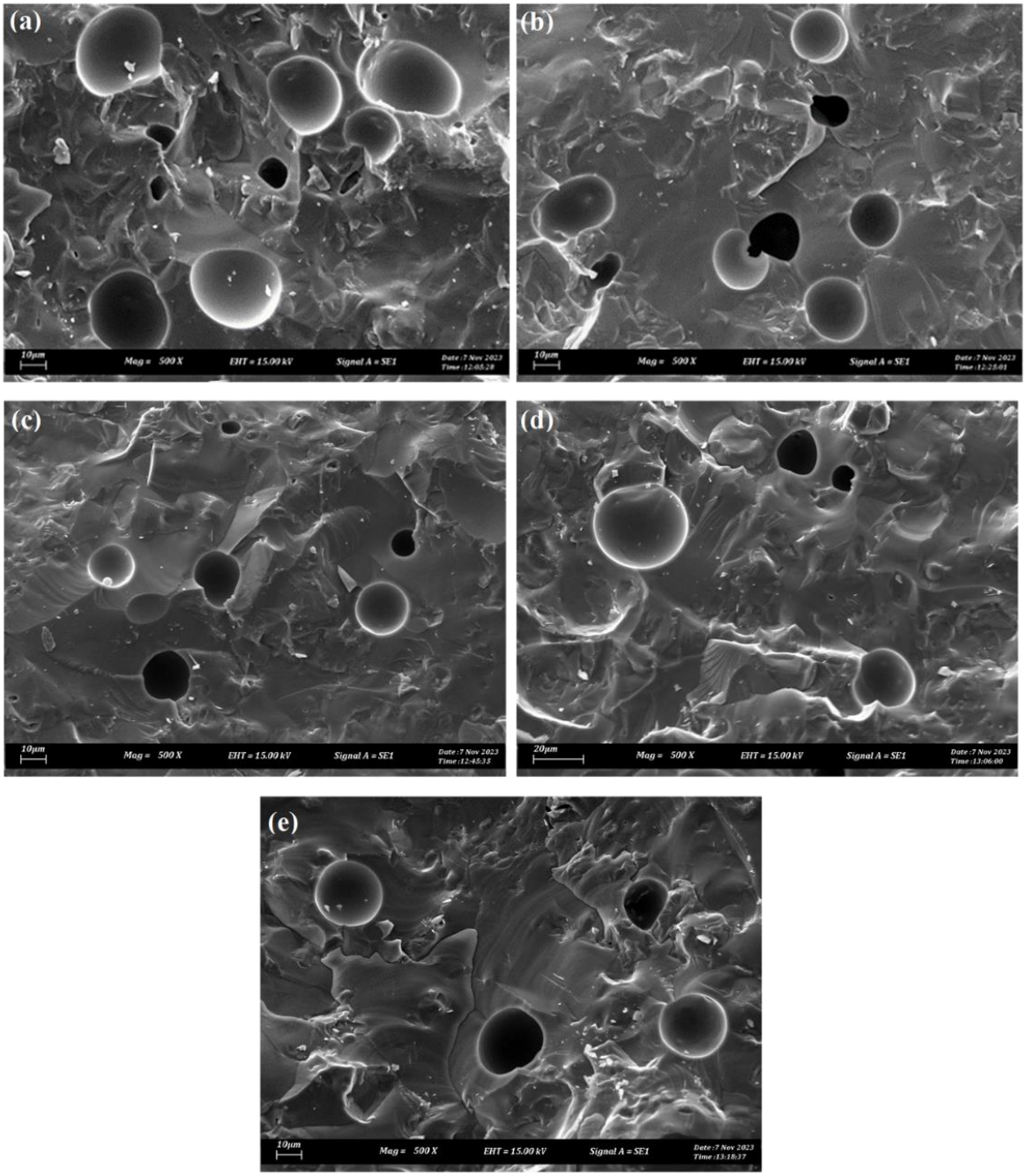

Figure 1: FESEM micrographs of dense porous ceramics with CB as the pore-forming agent at different concentrations: (a) 1 wt%, (b) 2 wt%, (c) 3 wt%, (d) 4 wt% and (e) 5 wt%

A significant decrease in average pore size is observed between 2 wt% and 3 wt%, which can be attributed to a densification effect during sintering. At moderate CB concentrations, localized densification may occur due to enhanced particle rearrangement, reducing pore coalescence and resulting in finer, more uniformly distributed pores. This trend is consistent with previous studies on porous zirconia ceramics, where a similar reduction in pore size at intermediate pore-forming agent concentrations was reported [15]. The measurement of average pore size was conducted using image analysis software, where high-resolution FESEM images were processed to identify and quantify pore diameters. A thresholding technique was employed to distinguish pore boundaries, followed by statistical averaging of the pore size distribution to derive mean values.

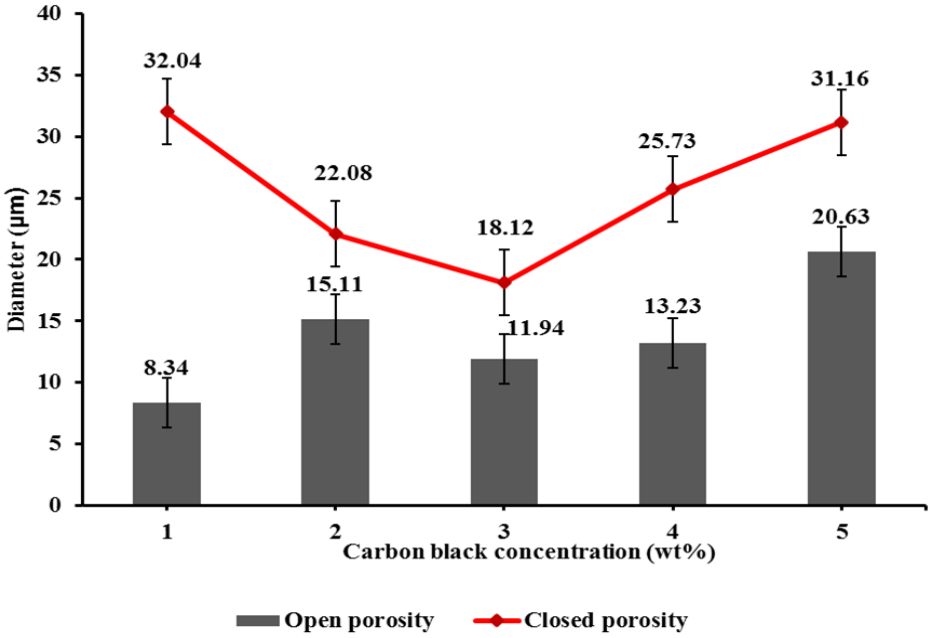

Figure 2: Average pore size for both open and closed pores in dense porous ceramics with CB as pore-forming agent

The utilization of PMMA as a pore-forming agent significantly influences the microstructural characteristics of porous ceramics. FESEM analysis, depicted in Figure 3, provides a detailed assessment of the morphological variations induced by different PMMA concentrations. In the absence of PMMA (0 wt%), the ceramic matrix maintains a dense structure with minimal porosity, establishing a fundamental reference for comparison. As PMMA content progressively increases from 1 wt% to 3 wt%, a substantial rise in both pore size and distribution is observed, confirming its role in enhancing porosity [16]. This phenomenon is primarily attributed to the thermal decomposition of PMMA during sintering, which results in the formation of well-defined voids within the ceramic matrix [17]. While these microstructural modifications are qualitatively evident, employing lower magnification imaging could further distinguish the pore morphology variations across different PMMA concentrations. The study highlights the critical impact of PMMA on the evolution of porosity, which has direct implications for optimizing thermal insulation and mechanical performance in ceramic applications [18].

The pore size distribution in porous ceramics plays a crucial role in determining their mechanical strength, permeability, and overall performance in various engineering applications. This study systematically examined the average pore size of both open and closed pores in dense porous ceramics fabricated with PMMA as a pore-forming agent at varying concentrations (1–5 wt%). Figure 4 illustrates the variation in average pore size for both open and closed pores in porous ceramics containing PMMA. An increasing trend in both pore types is observed with higher PMMA content. The findings indicate that increasing PMMA content leads to a progressive enlargement of open porosity, with the average pore diameter rising from 22.01 µm at 1 wt% to 32.35 µm at 5 wt%, while closed porosity exhibits a similar increasing trend from 13.68 µm to 25.53 µm. These results align with previous studies on PMMA-assisted porous ceramic fabrication, where PMMA microspheres have been reported to produce well-distributed pores with tunable sizes [16, 19]. The presence of interconnected open pores, particularly at higher PMMA concentrations, enhances permeability but compromises mechanical integrity, as demonstrated in porous zirconia and calcium hexaluminate ceramics [15, 20]. The hierarchical pore architecture formed using PMMA also contributes to improved thermal insulation properties and reduced bulk density [21, 22]. The findings of this study provide a fundamental framework for optimizing porosity distribution in porous ceramics, particularly for applications requiring a balance between mechanical robustness and permeability.

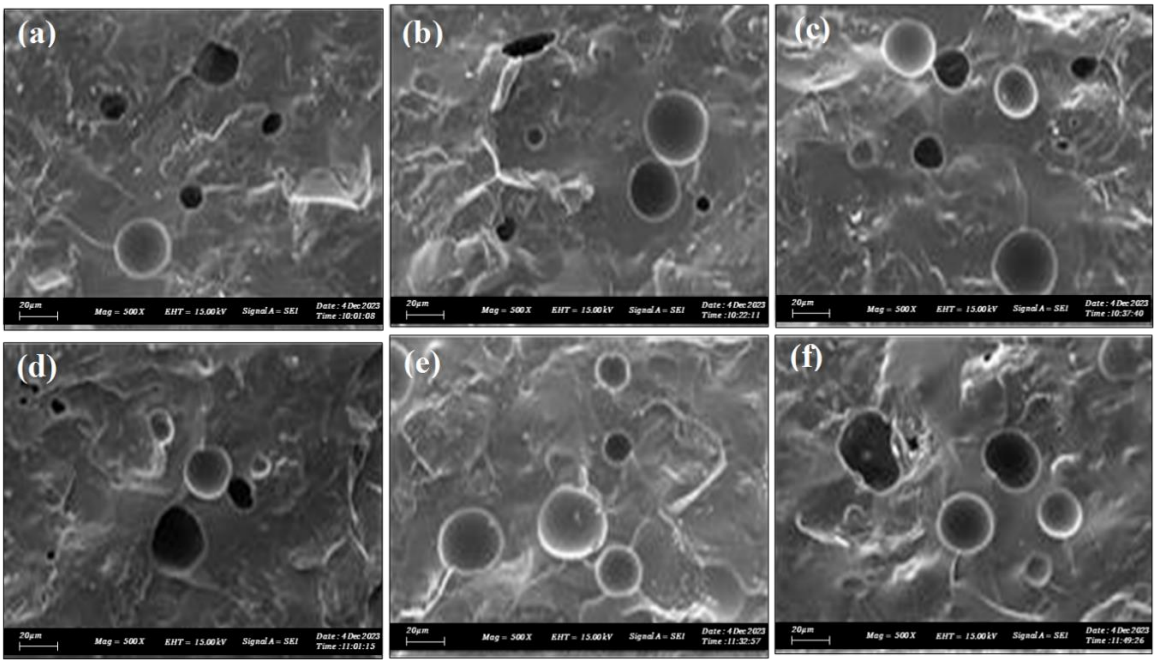

Figure 3: FESEM micrographs of dense porous ceramics at 500X magnification with PMMA as the pore-forming agent at different concentrations: (a) 0 wt%, (b) 1 wt%, (c) 2 wt%, (d) 3 wt%, (e) 4 wt% and (f) 5 wt%

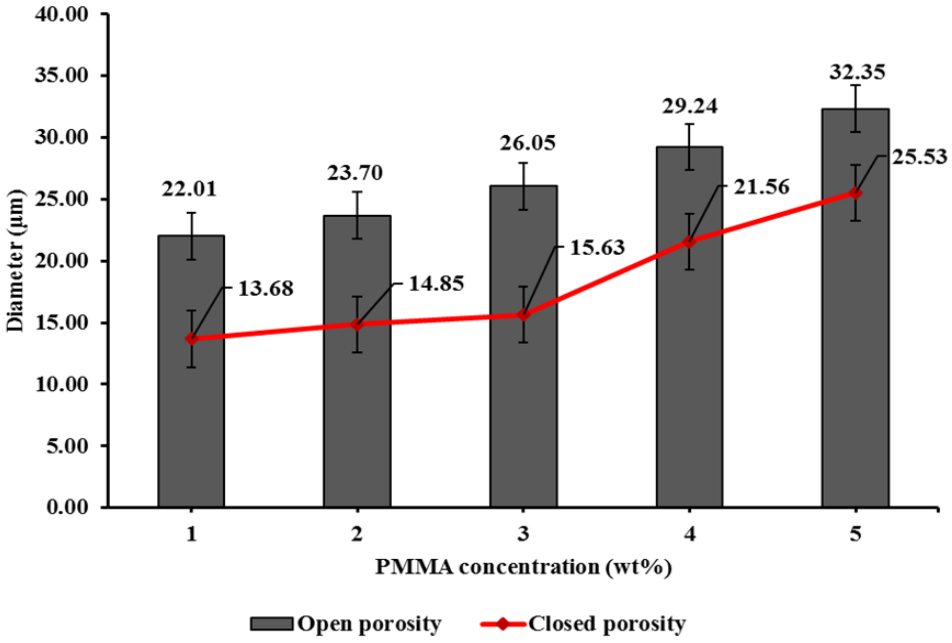

Figure 4: Average pore size for both open and closed pores in dense porous ceramics with PMMA as pore-forming agent

3.2 Phase Composition and Crystallographic Characterization of Porous Ceramics via XRD Analysis

The XRD patterns of dense porous ceramics prepared with varying CB contents (1–5 wt%) as a pore-forming agent are presented in Figure 5. The identified crystalline phases include orthoclase (O), silicon (Si), and mullite (M). The phase identification was confirmed using standard ICDD PDF card numbers. PDF card number 19-0932 data for orthoclase, PDF card number 46-1045 data for silicon

dioxide and PDF card number 15-0776 data for mullite. Notably, the diffraction peaks of orthoclase at approximately 27° exhibit an increase in intensity with rising CB content, suggesting a relative enhancement in crystallinity. However, contrary to the initial assumption, the systematic peak intensity variation across all compositions does not consistently support a general trend of increasing crystallinity for both orthoclase and silicon dioxide. The primary orthoclase reflections are recorded at 2θ values of 21.25°, 27.36°, 37.47°, and 42.05°, corresponding to diffraction planes (201), (202), (151), and (060), respectively. These findings align with prior studies that indicate the retention of orthoclase crystallinity in ceramic matrices subjected to thermal processing [4]. Furthermore, the decomposition of CB during sintering leads to enhanced porosity, as reported in similar works where CB acts as a volatile agent, promoting a porous structure within ceramics [23]. Nevertheless, this increase in porosity often results in reduced densification, which must be carefully considered for structural applications. The observed changes in peak intensity and phase composition suggest that CB addition affects the microstructural evolution of ceramics, influencing both crystallinity and porosity [24].

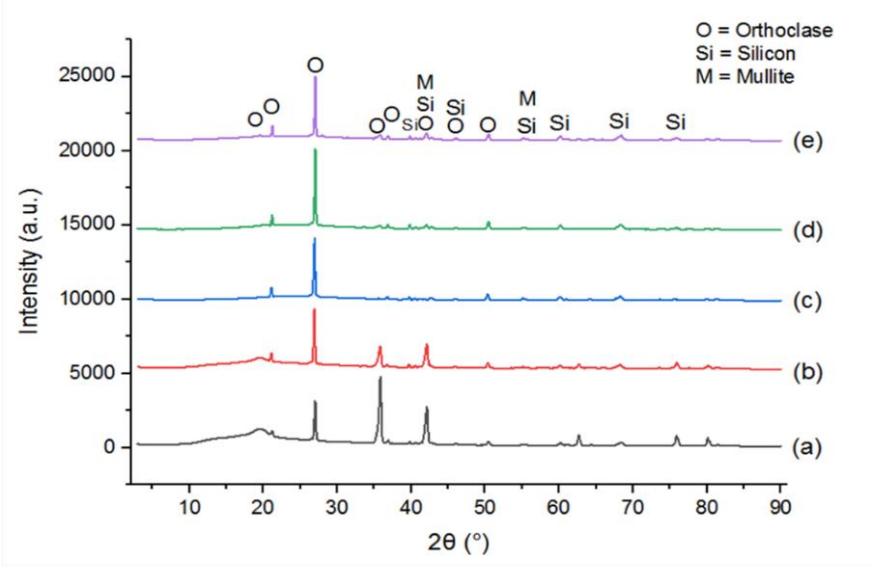

Figure 5: XRD patterns of dense porous ceramics with CB as pore-forming agent at various contents (a) 1 wt% (b) 2 wt% (c) 3 wt% (d) 4 wt% and (e) 5 wt%

Figure 6 presents the XRD patterns of dense porous ceramics synthesized with PMMA as a pore-forming agent at varying concentrations (0–5 wt%). The diffraction profiles reveal the presence of two dominant crystalline phases: orthoclase (O) and silicon (Si). Orthoclase, a feldspar mineral, and crystalline silica are critical constituents influencing the microstructural and mechanical integrity of ceramic materials. The diffraction peaks corresponding to orthoclase are observed at 38.20°, 44.43°, and 64.80°, while silicon peaks appear at 22.80°, 77.82°, and 82.00°. A systematic increase in peak intensity is evident with higher PMMA content, indicating an enhancement in crystallinity and phase formation within the ceramic matrix. This trend suggests that PMMA decomposition during sintering facilitates the evolution of porous microstructures, which in turn affects phase stability and material densification. Similar findings have been reported in previous studies where PMMA was employed as a sacrificial template to modulate porosity in ceramic systems [16, 20]. However, excessive porosity may compromise mechanical strength, necessitating an optimal balance between porosity and structural stability [25].

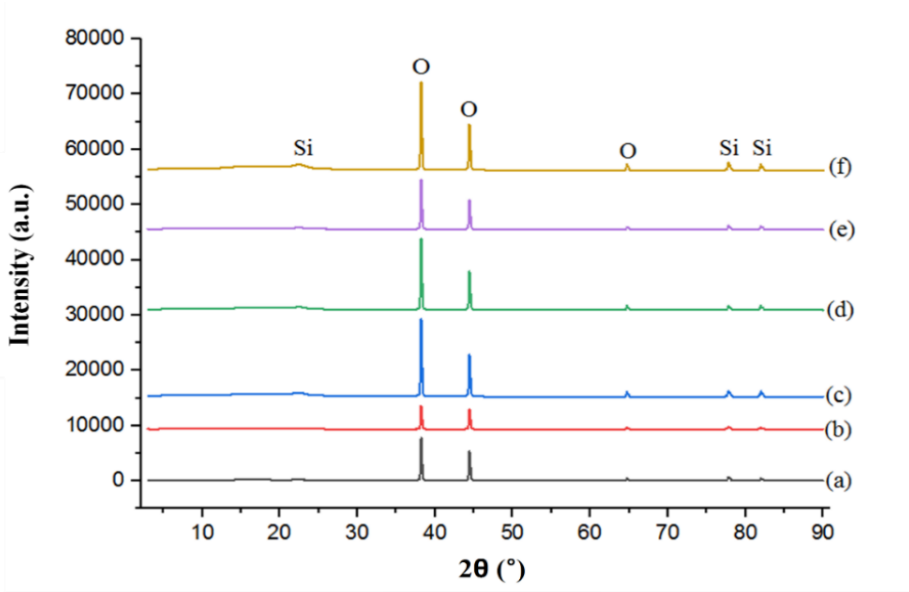

Figure 6: XRD patterns of dense porous ceramics with pmma as pore-forming agent at various contents (a) 0 wt% (b) 1 wt% (c) 2 wt% (d) 3 wt% (e) 4 wt% and (f) 5 wt%

The differences in XRD patterns between dense porous ceramics incorporating CB and PMMA as pore-forming agents arise from their distinct decomposition mechanisms and resultant porosity characteristics. CB, which decomposes at lower temperatures, predominantly leads to closed and small pores that minimally disrupt the crystalline lattice. As a result, ceramics fabricated with CB exhibit sharper and more intense diffraction peaks, indicating higher phase purity and crystallinity. In contrast, PMMA undergoes decomposition at elevated temperatures, generating larger interconnected open pores that induce strain and discontinuities within the crystalline lattice. This structural disruption is reflected in the XRD patterns as broader peaks with reduced intensity, signifying a decrease in crystallinity and a more heterogeneous phase distribution. Furthermore, the pore size variations significantly influence packing density and sintering behaviour, subsequently affecting phase stability and microstructural evolution [25]. Previous studies have demonstrated that controlled porosity enhances grain growth and phase clarity; however, the impact of different pore-forming agents on phase transformations at high temperatures remains an area requiring further exploration [6]. The observed disparities between CB and PMMA-derived ceramics highlight the necessity of optimizing pore morphology to balance porosity, mechanical integrity, and phase development for advanced ceramic applications [20]. A comprehensive understanding of the interplay between pore structure, sintering kinetics, and crystallization mechanisms is crucial for tailoring porous ceramics with enhanced functional properties.

3.3 Evaluation of Mechanical Properties: Flexural Strength and Porosity Influence

Flexural strength tests with three points were used to assess the mechanical characteristics of the sintered ceramic samples. The significant diversity, in flexural strength results could be attributed to variations in morphology and distribution, between PMMA and CB samples. The mechanical performance of porous ceramics is intricately linked to the type and concentration of pore-forming agents used during fabrication. Figure 7 illustrates the variation in flexural strength with increasing concentrations of CB and PMMA, highlighting the contrasting effects of these agents on the structural integrity of the ceramics. CB, known for its ability to create uniform, well-distributed pore structures, demonstrates superior mechanical performance compared to PMMA. The flexural strength of CB-incorporated ceramics exhibits a non-linear trend, peaking at 3 wt% with a maximum value of 49.72 MPa before decreasing at higher concentrations. This behaviour can be attributed to an optimal balance between porosity and load-bearing capability, where excessive CB content leads to interconnected voids that compromise mechanical integrity [4].

Conversely, the flexural strength of PMMA-containing ceramics shows a consistent decline with increasing PMMA content, dropping from 22.95 MPa at 1 wt% to 14.80 MPa at 5 wt%. This reduction is linked to the formation of larger, less uniform pores due to the thermal decomposition of PMMA during sintering, which results in higher porosity and weakened structural cohesion [16]. The observed trend aligns with previous studies, where pore-forming agents significantly impact the porosity-strength relationship in ceramics. For instance, the use of PMMA in porous alumina ceramics has been reported to decrease flexural strength due to increased pore size and volume fraction, reducing load transfer efficiency across the matrix [19]. In contrast, CB facilitates a finer and more interconnected pore network that enhances stress distribution and mitigates crack propagation, thereby contributing to improved mechanical robustness [12].

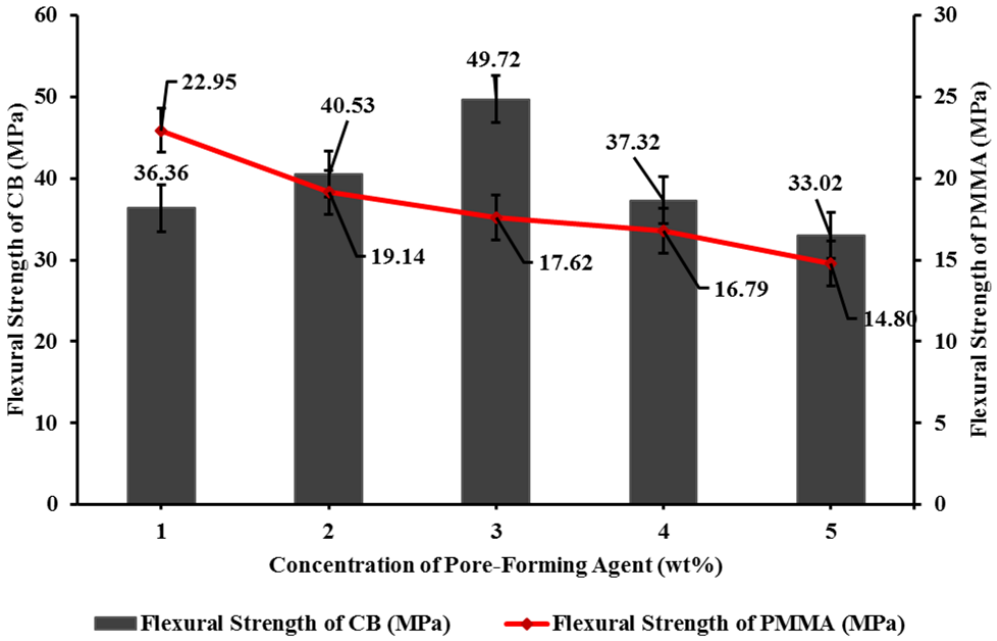

Figure 7: Flexural strength of dense porous ceramics with PMMA and CB as pore-forming agents

4. CONCLUSIONS

This study systematically investigated the morphological and mechanical properties of dense porous ceramics fabricated using CB and PMMA as pore-forming agents at varying concentrations (1–5 wt%). Microstructural analysis via FESEM demonstrated that CB generated small, uniformly distributed closed pores, thereby enhancing mechanical stability, whereas PMMA promoted larger, interconnected open pores, significantly increasing porosity at the expense of mechanical strength. XRD analysis confirmed the presence of orthoclase, silicon dioxide, and mullite phases, with crystallinity variations influenced by porogen type. The mechanical performance evaluation through three-point flexural testing established that 3 wt% CB yielded the highest flexural strength of 49.72 MPa, while PMMA incorporation at 5 wt% resulted in a reduced strength of 14.80 MPa due to excessive porosity and structural discontinuities. These findings underscore the critical role of porogen selection in tailoring ceramic microstructures, where CB proves advantageous for applications requiring high mechanical integrity, whereas PMMA is more suitable for applications prioritizing permeability and lightweight structures. The insights gained from this research contribute to the advancement of porous ceramics in energy-efficient insulation, filtration, and structural applications, providing a fundamental framework for optimizing the balance between porosity and mechanical strength in next-generation ceramic materials.

Acknowledgements

The authors extend their appreciation to the Skim Zamalah Universiti Teknikal Malaysia Melaka (UTeM), for funding this research work.

Author Contributions

All authors contributed toward data analysis, drafting and critically revising the paper and agree to be accountable for all aspects of the work.

Disclosure of Conflict of Interest

The authors have no disclosures to declare.

Compliance with Ethical Standards

The work is compliant with ethical standards.

References

[1] Chen, Y., Wang, N., Ola, O., Xia, Y. & Zhu, Y. (2021). Porous ceramics: Light in weight but heavy in energy and environment technologies. *Materials Science and Engineering: R: Reports*, 143, 100589.

[2] Lin, H., Shen, Q., Ma, M., Ji, R., Guo, H., Qi, H., Xing, W. & Tang, H. (2025). 3D printing of porous ceramics for enhanced thermal insulation properties. *Advanced Science*, 12(7), 2412554.

[3] Zhang, Y., Yu, L., Wang, J., Mao, H. & Cui, K. (2022). Microstructure and mechanical properties of high strength porous ceramics with high sewage sludge content. *Journal of Cleaner Production*, 380, 135084.

[4] Çelik, A., Çağlar, G. & Çelik, Y. (2022). Fabrication of porous Al_2O_3 ceramics using carbon black as a pore forming agent by spark plasma sintering. *Ceramics International*, 48(19), 28181-28190.

[5] Byun, Y. M., Lee, G. W., Lee, K. S., Park, J. G. & Kim, I. J. (2021). Mechanical properties of carbon fiber-reinforced Al_2O_3 porous ceramics. *Journal of the Korean Ceramic Society*, 58, 269-275.

[6] Yang, H., Li, Y., Li, Q., Wang, Z., Wu, H., Liu, X., Wu, Y. & Cheng, X. (2020). Preparation and properties of porous silicon nitride ceramics with polymethyl methacrylate as pore-forming agent. *Ceramics International*, 46(10), 17122-17129.

[7] Xu, H., Du, H., Kang, L., Cheng, Q., Feng, D. & Xia, S. (2021). Constructing straight pores and improving mechanical properties of GangueBased porous ceramics. *Journal of Renewable Materials*, 9(12), 2129-2141.

[8] Wang, L., An, L., Zhao, J., Shimai, S., Mao, X., Zhang, J., Liu, J. & Wang, S. (2021). High-strength porous alumina ceramics prepared from stable wet foams. *Journal of Advanced Ceramics*, 10(4), 852-859.

[9] Li, S., Zhang, H., Li, S., Wang, J., Wang, Q. & Cheng, Z. (2024). Advances in hierarchically porous materials: Fundamentals, preparation and applications. *Renewable and Sustainable Energy Reviews*, 202, 114641.

[10] Bowen, J. J., Mooraj, S., Goodman, J. A., Peng, S., Street, D. P., Roman-Manso, B., Davidson, E. C., Martin, K. L., Rueschhoff, L. M., Schiffres, S. N. & Dickerson, M. B. (2022). Hierarchically porous ceramics via direct writing of preceramic polymer-triblock copolymer inks. *Materials Today*, 58, 71-79.

[11] Hwang, J., Ejsmont, A., Freund, R., Goscianska, J., Schmidt, B. V. & Wuttke, S. (2020). Controlling the morphology of metal–organic frameworks and porous carbon materials: Metal oxides as primary architecture-directing agents. *Chemical Society Reviews*, 49(11), 3348-3422.

[12] Azlan, U. A. A., Jalaluddin, M. L., Borhanuddin, M. & Abd Rashid, M. W. (2024). Effect of carbon black content on morphological, crystalline phase, and mechanical characteristics of porous ceramic layers. *Malaysian Journal of Microscopy*, 20(1), 306-316.

[13] Chen, C., Ding, X., Wang, Y., Luo, Z. & Zhai, P. (2022). Fractal dimension analysis of structure and bending strength of porous alumina prepared using starch and carbon fiber as pore-forming agents. *Fractal and Fractional*, 6(10), 574.

[14] Fang, L., Chen, C. & Wang, Y. (2022). Carbon fibers and graphite as pore-forming agents for the obtention of porous alumina: correlating physical and fractal characteristics. *Fractal and Fractional*, 6(9), 501.

[15] Shen, J., Tian, X., Zhu, X., Liu, B., Jia, Q., Zhao, F. & Liu, X. (2022). Properties of porous zirconia ceramics fabricated by using various pore-forming agents. *Ceramics International*, 48(17), 25094-25102.

[16] Wang, S., Yang, Z., Luo, X., Qi, X., Zhang, L. & You, J. (2022). Preparation of calcium hexaluminate porous ceramics by gel-casting method with polymethyl methacrylate as pore-forming agent. *Ceramics International*, 48(20), 30356-30366.

[17] Aggarwal, M., Singh, A. K., Dhiman, S., Sharma, G., Thakur, O. P. & Kumar, S. (2022). Microstructural tuning: A route towards realization of enhanced pyroelectric figure of merits of Sr and Zr doped barium titanate ceramics. *Materials Today Communications*, 31, 103302.

[18] Zhu, Y., Guo, B., Zuo, W., Jiang, K., Chen, H. & Ku, J. (2022). Effect of sintering temperature on structure and properties of porous ceramics from tungsten ore tailings. *Materials Chemistry and Physics*, 287,126315.

[19] Wu, R., Zeng, T., Fan, M., Cui, Y., Xu, G., Wang, X., & Cheng, S. (2023). Microstructure and mechanical properties of 3D printed porous Al2O3–ZrO2 laminated ceramics with tailored porosity. *Ceramics International*, 49(20), 33369-33381.

[20] Jalaluddin, M. L., Azlan, U. A. A., Abd Rashid, M. W., Tamin, N., & Masri, M. N. (2024). A review of pore-forming agents on the structures, porosities, and mechanical properties of porous ceramics. *AIMS Materials Science*, 11(4), 634-665.

[21] Dai, Y. L., Yao, D. X., Xia, Y. F., Zhu, M., Zhao, J., Wang, F. & Zeng, Y. P. (2025). Fabrication of hierarchical porous si_3n_4 ceramics by direct ink writing combined with pore forming agent. *Materials Today Communications*, 45, 112204.

[22] Dele-Afolabi, T. T., Hanim, M. A., Oyekanmi, A. A., Ansari, M. N. M., Sikiru, S. & Ojo-Kupoluyi, O. J. (2024). Organic waste-derived pore formers for macroporous ceramics fabrication: A review on synthesis, durability properties and potential applications. *Materials Today Sustainability*, 100824.

[23] Huang, Y., Hu, N., Ye, Y., Ou, Z. & Shi, X. (2022). Preparation and pore-forming mechanism of $MgO–Al_2O_3–CaO$-based porous ceramics using phosphorus tailings. *Ceramics International*, 48(20), 29882-29891.

[24] Jalaluddin, M. L., Azlan, U. A. A. & Rashid, M. W. A. (2023). A preliminary study of porous ceramics with carbon black contents. *AIMS Materials Science*, 10(5), 741-754.

[25] Wu, Y. R., Tian, C., Wu, J. M., Huang, H. L., Liu, C. L., Lin, X., Cheng, L. J. & Shi, Y. S. (2023). Influence of the content of polymethyl methacrylate on the properties of porous Si_3N_4 ceramics fabricated by digital light processing. *Ceramics International*, 49(19), 31228-31235.